

Supporting Information

Exploring a New Class of Singlet Fission Fluorene Derivatives by Unveiling the Role of Intramolecular Charge Transfer

Letizia Mencaroni, Benedetta Carlotti,* Fausto Elisei, Assunta Marrocchi, Anna Spalletti

Department of Chemistry, Biology and Biotechnology and CEMIN, University of Perugia, via Elce di Sotto 8, 06123, Perugia, Italy.

List of Contents

1. Experimental methods
2. Synthesis and characterization of compound **F**
3. Photophysical properties
 - 3.1 Spectral properties
 - 3.2 Phosphorescence measurements
 - 3.2.1 Singlet oxygen phosphorescence
 - 3.2.2 Phosphorescence spectrum of compound **F**
 - 3.3 Nanosecond transient absorption measurements
 - 3.3.1 Determination of the triplet energy by sensitization
 - 3.3.2 Determination of the triplet absorption coefficient
 - 3.3.3 Determination of the triplet quantum yields
 - 3.3.4 Concentration effect on the triplet quantum yields
 - 3.4 Femtosecond transient absorption experiments
4. Quantum mechanical calculations
5. References

1. Experimental methods

Chemicals. The synthetic procedures of **AF** (2-[(3,4-(bis(esiloxy)-phenylethynyl),7-(4-aldehyde-phenylethynyl)] fluorene) and **NF** (2-[(3,4-(bis(dodeciloxy)-phenylethynyl),7-(4-nitro-phenylethynyl)] fluorene) compounds had been already described in a previous paper.¹ For compound **F** (2,7-bis[3,4-bis(dodeciloxy)-phenylethynyl] fluorene) the synthesis is reported below in the dedicated paragraph.

Spectral and photophysical characterizations were performed in several solvents of spectroscopic grade: cyclohexane (CH, VWR Chemicals), methyl cyclohexane (MC, ACS Reagent, Sigma-Aldrich), 3-methyl pentane (3MP, Acros Organics), toluene (Tol, ACS Reagent, Sigma-Aldrich), ethyl acetate (EtAc, AnalaR, BDH), dichloromethane (DCM, Carlo Erba Reagents), dimethylformamide (DMF, ACS Reagent, Sigma-Aldrich) and acetonitrile (MeCN, VWR Chemicals).

Photophysical measurements. Absorption spectra of solutions ($\approx 1 \times 10^{-5}$ M) were recorded by using a Cary 4E (Varian) spectrophotometer. Fluorescence and excitation spectra were instead detected by a FluoroMax-4P spectrofluorimeter (HORIBA Scientific) and manipulated by FluorEssence software with the appropriate instrumental response corrections. The fluorescence quantum yields (Φ_F , experimental error $\pm 10\%$ and $\pm 20\%$ when $\Phi_F < 10^{-4}$) of dilute solutions (1×10^{-6} M) were obtained exciting each sample at the relative maximum absorption wavelength by employing 9,10-diphenylanthracene ($\Phi_F = 0.73$ in air-equilibrated cyclohexane)² as reference compound. The concentration effect on fluorescence properties of compound **AF** was addressed by a Spex Fluorolog-2 F112AI spectrofluorimeter in front-face configuration.

Singlet oxygen in air-equilibrated solution ($\approx 1 \times 10^{-5}$ M) was produced by sensitization experiments from the three fluorene derivatives in CH and Tol. The $^1\text{O}_2$ phosphorescence spectra was detected through a spectrofluorimeter FS5 (Edinburgh Instrument) equipped with a InGaAs detector. Phenalenone ($\Phi_{\Delta} = 0.95$ in CH and 0.99 in Tol) was used as reference compound for comparison purpose.³ The same spectrofluorimeter was employed to acquire the phosphorescence spectra of compound **F** in the glass matrix constituted by methyl-cyclohexane and 3-methyl-pentane (MC-3MP), 9/1 v/v ratio, at 77K by exciting the sample at the maximum absorption wavelength with a microsecond pulsed lamp with tunable excitation frequency (from 40Hz to 0.25Hz).

Triplet properties were measured by laser flash photolysis (Edinburgh LP980) with a pump pulse centered at 355 nm (third harmonic of a Continuum Surelite II Nd:YAG laser, Spectra Physics) with nanosecond time-resolution (pulse width 7 ns and laser energy < 1 mJ pulse⁻¹) coupled with a PMT for signal detection. A pulsed xenon lamp was then used to probe the absorption properties of the produced excited states. Energy transfer experiments in de-aerated conditions have been exploited in order to acquire the sensitized triplet transient absorption spectra and in particular to experimentally determine the triplet energy, employing a wide selection of sensitizers of known triplet energy, acting both as donors and acceptors, and deriving the quenching kinetic constants. The detailed procedure can be found in the relative paragraph (Section 3.3.1). Triplet-triplet absorption coefficients (ϵ_T) were taken from ref. ¹ and measured in the case of the newly-synthesized compound by energy transfer experiments (see below Section 3.3.2) from **F** to the all-trans- α , ω -di(2-thienyl)octatetraene (**D2TO**, $\Phi_T < 0.005$ and $\epsilon_T = 53000$ M⁻¹ cm⁻¹ at 465 nm)⁴ in CH. An actinometry approach, deepened in Section 3.3.3, was then used to measure the triplet quantum yields considering Thioxanten-9-one (**TX**) in MeCN ($\Phi_T = 0.66^5$ and $\epsilon_T = 30000$ M⁻¹ cm⁻¹ at 630 nm⁶ and anthracene (**A**) in CH ($\Phi_T = 0.71$ and $\epsilon_T = 45500$ M⁻¹ cm⁻¹ at 422 nm)⁷ as references with known Φ_T and ϵ_T values. The uncertainties were estimated to be about $\pm 15\%$ on Φ_T and $\pm 10\%$ in the product $\Phi_T \times \epsilon_T$. All measurements were performed by purging the sample with pure nitrogen. The study of the concentration effect on Φ_T was intrinsically limited by the experimental technique. Therefore, a narrow range of concentrations (corresponding to absorbances: $A_{355} \approx 0.1, 0.3, 0.5$ up to $A_{355} = 1$, condition of total absorbance) was analyzed (see dedicated Section 3.3.4).

The experimental setup for the femtosecond transient absorption and fluorescence up-conversion measurements have been widely described elsewhere ⁸⁻¹¹. Particularly, the 800-nm radiation is amplified by the Ti:Sapphire laser system (Spectra Physics) and, successively, converted into the 266 and 400-nm excitation pulses (ca. 60 fs) by Apollo (2nd and 3rd Harmonic generator). A small portion of the fundamental laser beam (800 nm light) enters the transient absorption spectrometer (Helios, Ultrafast Systems), passes through an optical delay line (time window of 3200 ps) and is finally focused onto a Sapphire crystal (2 mm thick) to generate a white-light continuum (450–800 nm), used as probe. The temporal resolution is about 150 fs and the spectral resolution 1.5 nm. In the Up-Conversion set up (Halcyone, Ultrafast System), the 400-nm pulse excites the sample whereas the fundamental laser beam acts as the “gate” light, after passing through a delay line, which is then summed to the sample emission promoting the up-conversion process. The time resolution is about 200 fs while the spectra resolution is 1.5 nm. Most measurements were carried out under the magic angle condition in a 2-mm cell considering $0.5 < A < 1$ at λ_{pump} (ca. 1×10^{-4} M). We have employed a 400 nm pump for **NF** and **AF**, as this wavelength is at the red-edge of their absorption spectra; a 266 nm pump was used for **F** as this sample shows negligible absorption at 400 nm. The solution was stirred during the experiments to avoid photoproduct interferences. Photodegradation was checked recording the absorption spectra before and after the time-resolved measurement, where no significant change was observed. The experimental 3D data matrixes were firstly analyzed performing the Global Analysis by Surface Xplorer PRO (Ultrafast Systems) software, and successively through GloTarAn software in order to obtain the Evolution-Associated Spectra (EAS) considering a consecutive kinetic model. The SF mechanism was then detailed by running the Target Analysis with the same software, considering consecutive and parallel steps to describe the evolution of transients providing the Species Associated Spectra (SAS).^{12,13}

Quantum mechanical calculations. Energy level diagram, including the first electronic excited singlet and triplet states, was predicted by quantum mechanical calculations using the Gaussian 16 package ¹⁴. CAM-B3LYP have been chosen as method to perform both S_0 , S_1 and T_1 geometry optimization and to draw the theoretical absorption spectra by employing DFT and TD-DFT levels of theory for these small organic push-pull systems.¹⁵ Every calculation was submitted setting 6-31g+G(d,p) as basis set including the solvent effect (cyclohexane) according to the conductor-like polarizable continuum model (CPCM) ¹⁶. Vertical, $E(S_1)_{\text{FC}} = E(S_1, S_0) - (E(S_0, S_0))$ and $E(T_1)_{\text{FC}} = E(T_1, S_0) - (E(S_0, S_0))$, and adiabatic, $E(S_1)_{\text{REL}} = E(S_1, S_1) - (E(S_0, S_0))$ and $E(T_1)_{\text{REL}} = E(T_1, T_1) - (E(S_0, S_0))$, energy gaps have been considered when verifying the feasibility of

SF according to the principal energy criterion ($E(S_1) \geq 2T_1$) and establishing the thermodynamic of the process: $\Delta E_{S-TT} = 2E(T_1, REL) - E(S_1, FC)$.

2. Synthesis and characterization of F

2,7-bis[3,4-bis(dodeciloxy)-phenylethynyl] fluorene: Dry toluene (6 ml), dibromofluorene (1.1 mmol), CuI (0.02 mmol), Pd(PPh₃)₄ (0.02 mmol) and diisopropylamine (3 ml) were placed in a reactor and degassed under inert atmosphere at 0 °C. Dodecyloxy-4-ethynylbenzene (2 mmol) was then added and the mixture was kept at 75 °C (20h). Next, the solvent was fully evaporated, and the crude reaction mixture was purified by column chromatography (silica gel, petroleum ether/dichloromethane 4:1). Yield: 62%.

¹H NMR (CDCl₃) δ : 7.80–7.56 (m, 6H), 6.91–6.86 (m, 4H), 6.62 (m, 2H), 3.95 (m, 10H), 1.75 (m, 8H), 1.38–1.21 (m, 72H), 0.89 (m, 12H).

3. Photophysical properties

3.1 Spectral properties

Table S1. Molar absorption coefficients of the ground state (ϵ_G) of compounds **F**, **AF** and **NF** in CH.

	F	AF	NF
λ_G / nm	329	368	376
$\epsilon_G / \text{M}^{-1}\text{cm}^{-1}$	49500	46900	52000

Table S2. Comparison between spectral and fluorescence properties of **F**, **AF** and **NF** in solvents of different polarity: maximum absorption wavelength (λ_{abs}), maximum emission wavelength (λ_{em}), Stokes Shift ($\Delta\nu$) and fluorescence quantum yield (Φ_F).

	F				AF				NF			
	$\lambda_{\text{abs}} / \text{nm}$	$\lambda_{\text{em}} / \text{nm}$	$\Delta\nu / \text{cm}^{-1}$	Φ_F	$\lambda_{\text{abs}} / \text{nm}$	$\lambda_{\text{em}} / \text{nm}$	$\Delta\nu / \text{cm}^{-1}$	Φ_F	$\lambda_{\text{abs}} / \text{nm}$	$\lambda_{\text{em}} / \text{nm}$	$\Delta\nu / \text{cm}^{-1}$	Φ_F
CH	325 , 348	385	2760	0.03	364	397	2280	0.37	370	418	3100	0.0003
Tol	329 , 353	392	2820	0.04	367	412	2980	0.15	373	478	5890	-
EtAc	327 , 349	390	3010	0.05	361	456	5770	0.32	366	563	7940	0.0035
DMF	329 , 353	420	4520	0.08	364	520	8240	0.002	370	-	-	<0.0001

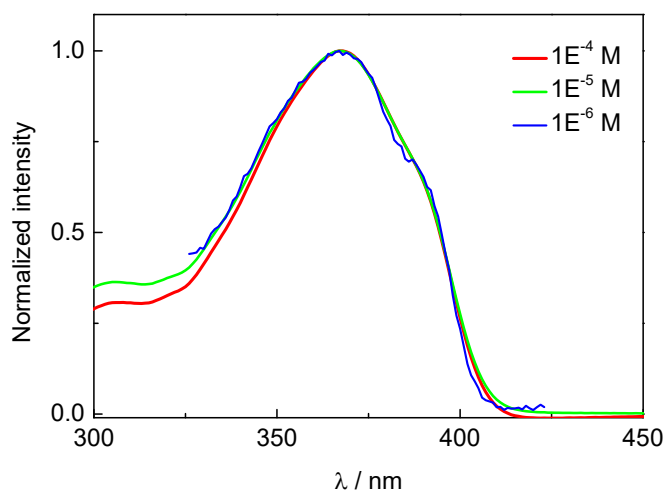


Figure S1. Concentration effect on absorption spectra of **AF** in Tol.

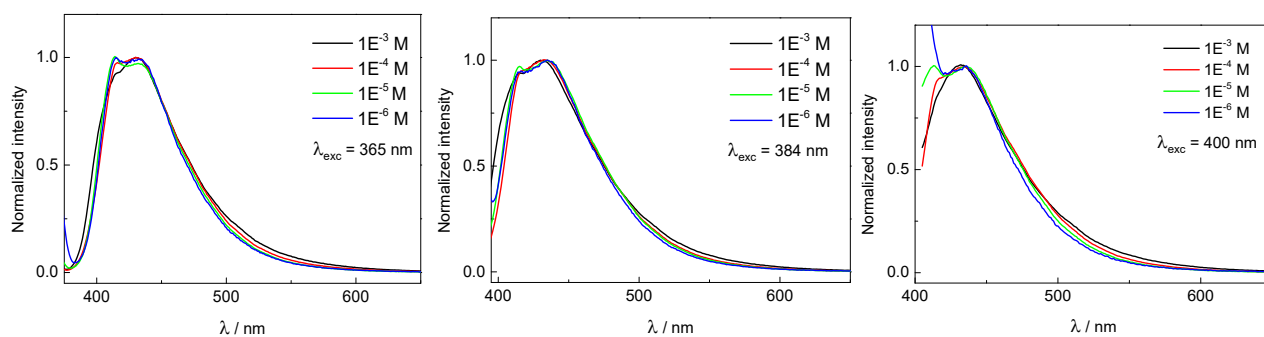


Figure S2. Concentration effect on fluorescence spectra of **AF** in Tol at different excitation wavelengths ($\lambda_{\text{exc}} = 365, 384, 400$ nm, respectively from the left panel to the right panel).

3.2 Phosphorescence measurements

3.2.1 Singlet oxygen phosphorescence

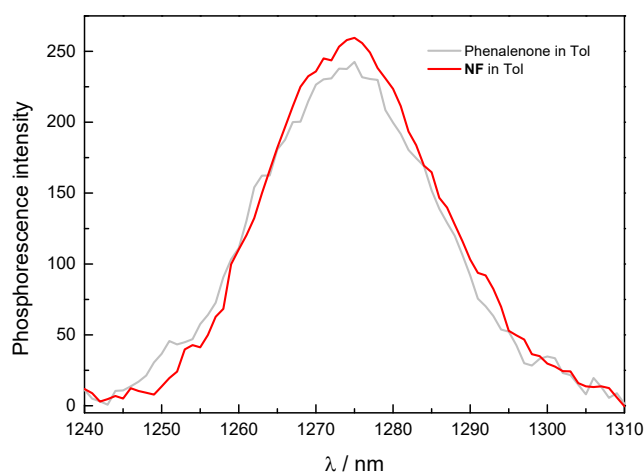


Figure S3. Comparison between phosphorescence spectra of singlet oxygen produced by **NF** (red) and phenalene (gray) in toluene solution (ca. 1×10^{-5} M) for comparison. The spectra are recorded in the same experimental conditions including slits width and absorbance value (ca. 0.6) at the excitation wavelength, being the maximum absorption wavelength.

3.2.2 Phosphorescence spectrum of compound F

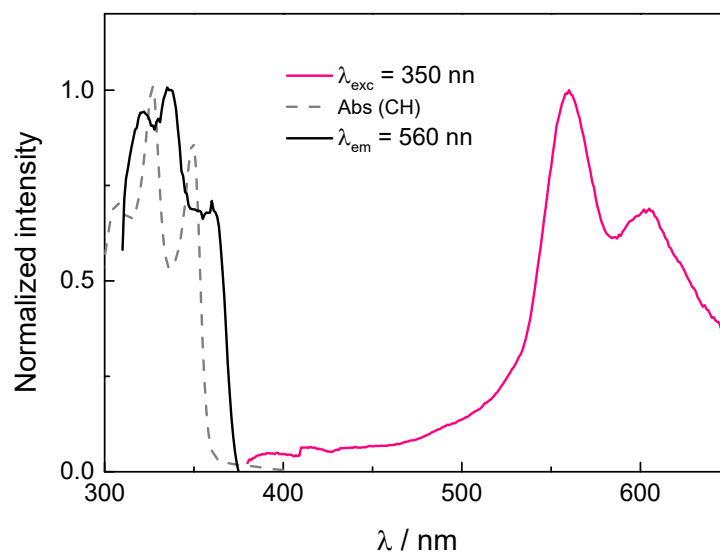


Figure S4. Phosphorescence spectrum of compound F in MC-3MP matrix (pink line) obtained by exciting the sample (3×10^{-5} M) at 350 nm by 10Hz pulsed lamp at 77 K. The phosphorescence excitation spectrum (black line) and the absorption spectrum in CH at room temperature (dashed line) are also shown.

3.3 Nanosecond transient absorption measurements

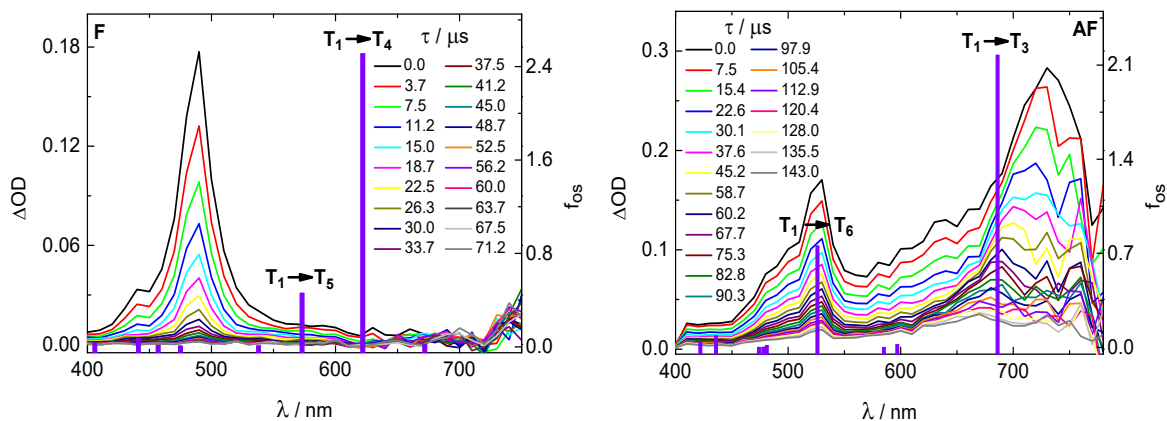


Figure S5. Transient absorption spectra of F (left) and AF (right) in de-aerated CH (ca. 1×10^{-5} M) obtained by ns flash photolysis experiments ($\lambda_{exc} = 355$ nm) and theoretical triplet absorption spectra (violet bars) obtained by quantum mechanical calculations.

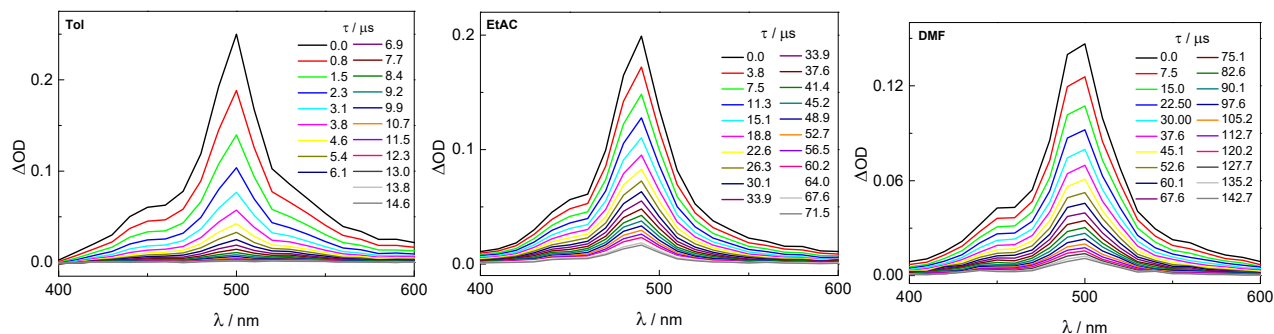


Figure S6: Triplet transient absorption spectra of compound F (ca. 1×10^{-5} M) in solvents of different polarity obtained by ns flash photolysis experiments ($\lambda_{exc} = 355$ nm) in de-aerated conditions.

3.3.1 Determination of the triplet energy by sensitization

The determination of the triplet energy via sensitization was achieved by energy transfer experiments from many energy donors (Acetophenone, **Acph**, thioxanthene-9-one, **TX**, 2,2-bisthienylketone, **DTK**, 2'-Acetonaphthone, **2-AcNph**, Chrysene, **Cry**, 1'-Acetonaphthone, **1-AcNaph**, 1-Naphthaldehyde, **1-Naph**, 2,3-Butanedione, **Byl**, and 7H-Benz(a)anthracen-7-one, **7BAone**) in DCM and several acceptors (Pyrene, **Pyr**, **7Baone**, 2,4-Pentandione Iron(III) derivative, **2,4PDI**, Anthracene, **A**, and **D2TO**) in CH.^{2,4,17-19} When using the fluorene molecules as acceptors, the solvent was conveniently chosen considering the reduced triplet quantum yield of the fluorene derivatives in a polar environment such as DCM, thus limiting the direct excitation of the acceptor, and to avoid the hydrogen abstraction affecting DMF solutions. Acetonitrile was also excluded due to solubility issues. The experimental procedure starts from recording the kinetics corresponding to the triplet absorption maxima (λ_T) of the solution containing the donor alone ($A_D \approx 0.9$ at 355 nm), in order to obtain its triplet lifetime (τ_D). Then, donor/acceptor mixtures ($A_{TOT} = A_D + A_Q \approx 1.1$) have been analyzed by recording the kinetics in correspondence of the donor and acceptor maximum wavelengths and fitted, accounting for the shorter lifetime of the quenched donor (τ_{D+A}) or the rise-decay dynamics at the λ_T of the acceptor, being the body of proof of the accomplished energy transfer. The transient absorption spectra of the donor/acceptor mixtures were also acquired. To avoid any inaccuracy, in the cases where the ESA signals of the energy donor were found to be substantially overlapped to those of the acceptor, the rise time at the λ_T of the acceptor has rather been considered. Triplet lifetimes of the donor (τ_D) and quenched donor (τ_{D+A}), together with the concentration of the acceptor ($[Q]$) have been manipulated in the well-known Stern-Volmer equation (Eq. 1) for the calculation of the quenching constants (k_q):

$$\frac{\tau_D}{\tau_{D+A}} = 1 + k_q \cdot [Q]$$

Eq.1

The energy transfer experiments from **DTK** in DCM ($\lambda_T = 630$ and 400 nm) to the fluorene derivatives and from fluorenes ($\lambda_T = 490, 530$ nm) to **Pyr** in CH ($\lambda_T = 422$ nm) are shown in detail as representative examples (Figures S7-S9).

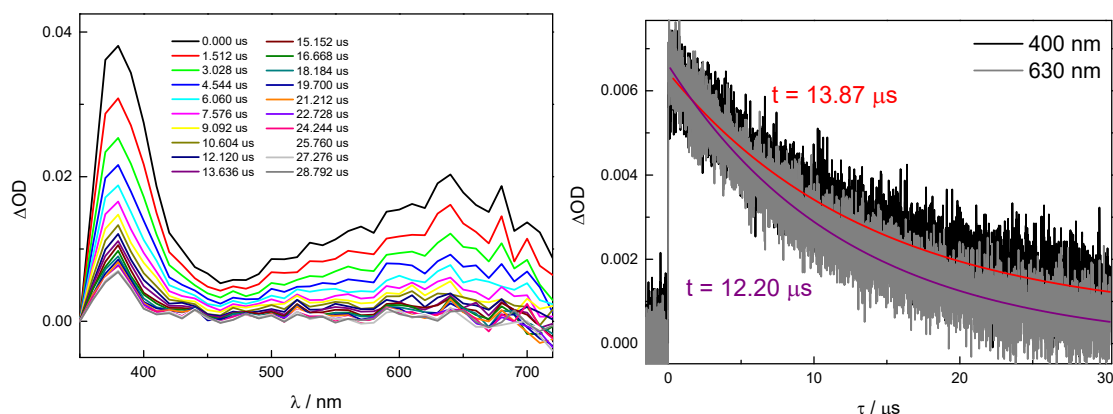


Figure S7: Transient triplet absorption spectrum (left) and representative kinetics (right) of **DTK** in DCM obtained by ns flash photolysis ($\lambda_{exc} = 355$ nm) in de-aerated conditions.

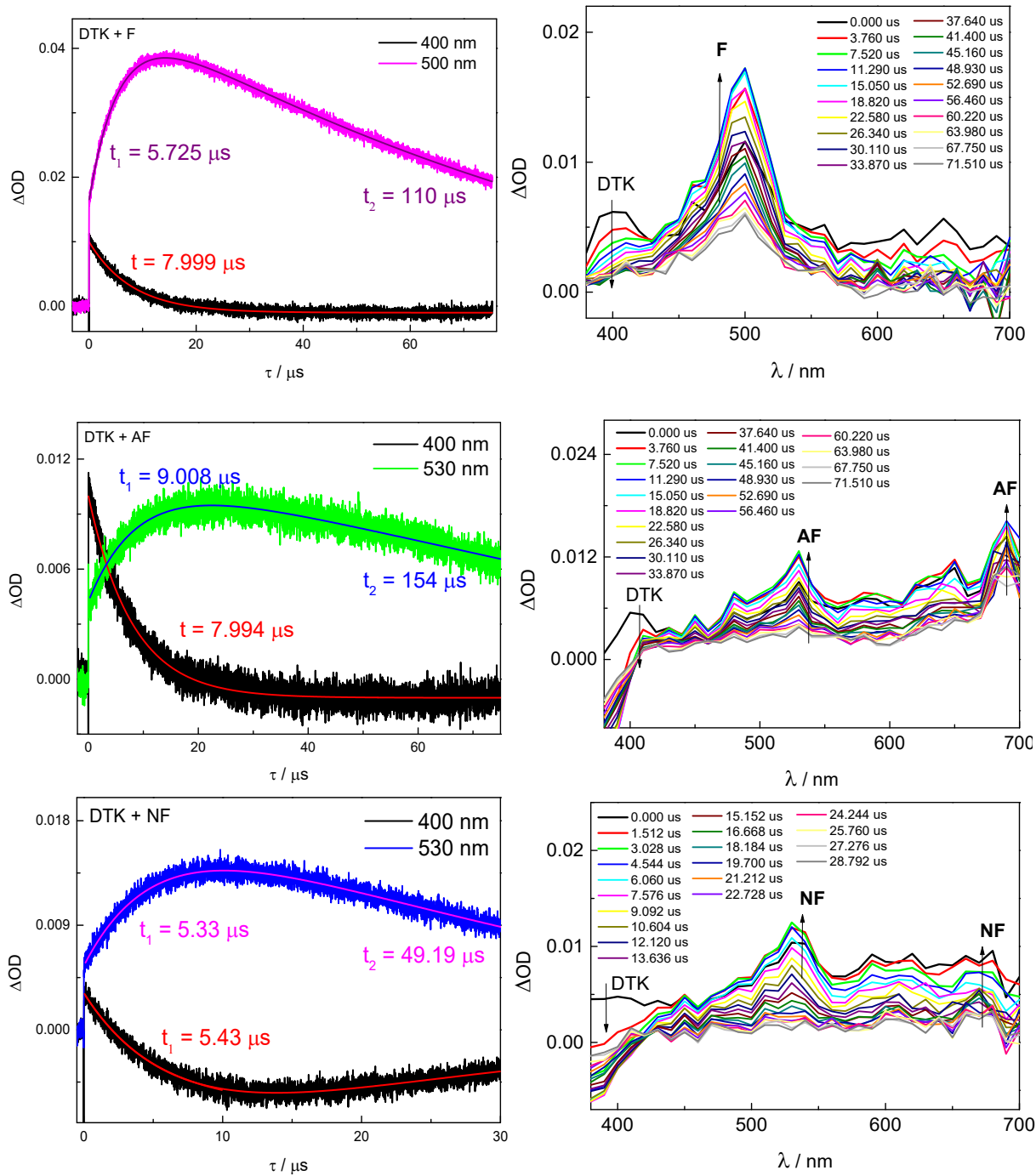


Figure S8: Kinetics (left panels) and transient absorption spectra (right panels) of **DTK/F**, **DTK/AF** and **DTK/NF** mixtures in DCM obtained by ns flash photolysis ($\lambda_{exc} = 355$ nm) in de-aerated conditions.

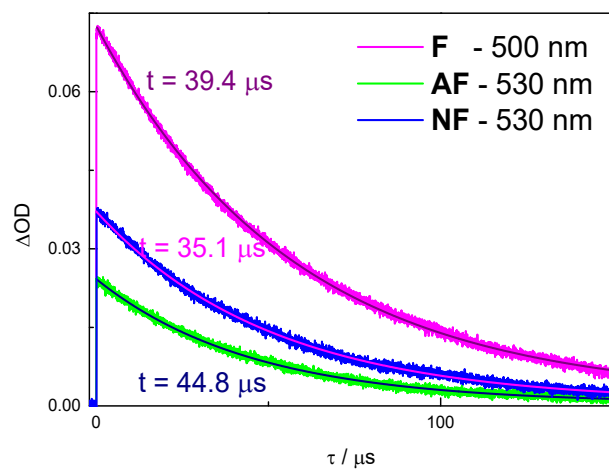


Figure S9: Kinetics recorded at λ_{τ} of fluorene derivatives in CH obtained by ns flash photolysis ($\lambda_{exc} = 355$ nm) in de-aerated conditions.

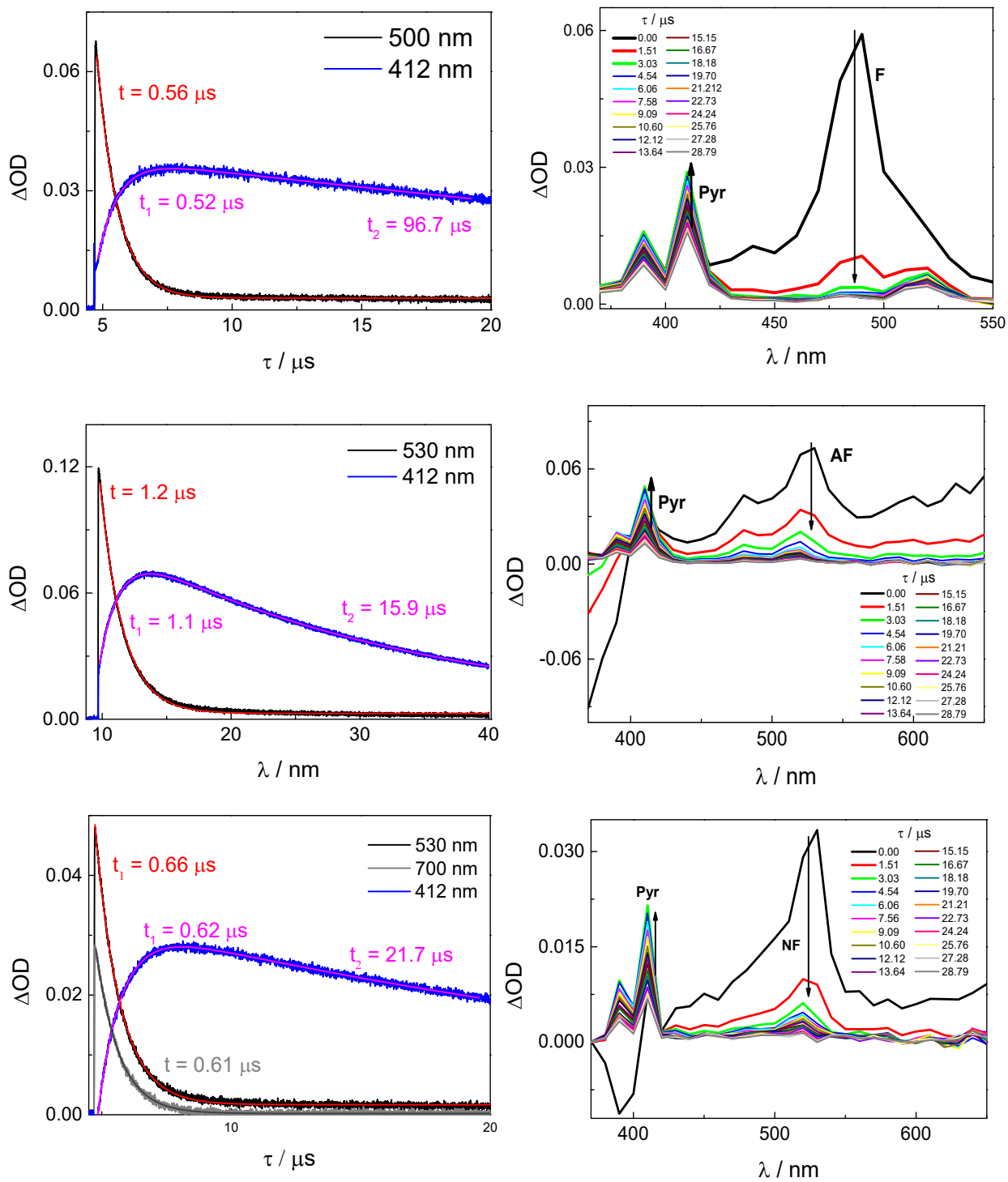


Figure S10: Representative kinetics (left panels) and transient absorption spectra (right panels) of F/Pyr, AF/Pyr and NF/Pyr mixtures in CH obtained by ns flash photolysis ($\lambda_{exc} = 355$ nm) in de-aerated conditions.

Generally, in all cases the quenching constant values, obtained through Eq.1, are in line with the diffusional constants in the investigated solvents at 20 °C² when considering sensitizers with $E_T \geq 2.44$ eV (**1-NphA**) in DCM ($k_q \sim 3 \times 10^{10} \text{ M}^{-1} \text{ s}^{-1}$). In addition, the fluorene derivatives act as efficient sensitizers, with a diffusional rate ($k_q \sim 3 \times 10^9 \text{ M}^{-1} \text{ s}^{-1}$), when the $E_T \leq 1.85$ eV, namely when using **A** as acceptor in CH solutions. As a consequence, the unknown triplet energies of our samples are comprised between 2.44 and 1.85 eV, pointing out that Pyrene (2.12 eV) and 7H-Benz(a)anthracen-7-one (2.04 eV) represent the crucial experiments and for this reason are reported in detail for all the investigated fluorene compounds in Table S4.

Table S3: Comparison between quenching constants ($k_q, \text{M}^{-1} \text{s}^{-1}$) of fluorene derivatives.

	1-Naph (Donor)	Pyr (Acceptor)	7BAone (Acceptor)	A (Acceptor)
E_T / eV	2.44	2.12	2.04	1.85
F	5.18E+09	9.94E+07	9.90E+08	2.65E+09
AF	2.93E+09	5.48E+06	1.68E+09	1.65E+09
NF	1.29E+09	2.61E+07	1.74E+09	4.47E+09

Based on these data, we can derive the following conclusions about the triplet energies as obtained from the experiments:

- Surprisingly, the k_q values found for Fluorenes to **Pyr** perfectly reproduce the E_T trend as obtained by TD-DFT calculations: **F** > **NF** > **AF**, as evidenced by the lowest quenching constant for **AF/Pyr** in CH. A more activated, and then slower, energy transfer process occurs due to the lower triplet energy of **AF** ($5.5 \times 10^6 \text{ M}^{-1} \text{s}^{-1}$) if compared to **NF** ($2.6 \times 10^7 \text{ M}^{-1} \text{s}^{-1}$) and **F** ($1.0 \times 10^8 \text{ M}^{-1} \text{s}^{-1}$). As for **AF**, $E_T < 2.12$ eV.
- **F**: considering the phosphorescence spectrum peaked at 560 nm (2.21 eV) in MC-3MP and the low quenching constant of about $1 \times 10^8 \text{ M}^{-1} \text{s}^{-1}$ in the case of **F/Pyr** in CH, the triplet energy reasonably lies between 2.21 and 2.12 eV.
- **NF**: the analogous values of k_q when considering **7BAone/NF** in DCM ($1.3 \times 10^9 \text{ M}^{-1} \text{s}^{-1}$) and **NF/7BAone** in CH ($1.7 \times 10^9 \text{ M}^{-1} \text{s}^{-1}$) suggest that $E_T \approx 2.04$ eV.

3.3.2 Determination of the triplet absorption coefficient trough energy transfer experiments

The determination of the triplet absorption coefficient (ε_T) is provided by energy transfer experiments from the donor (compound **F**) to the energy acceptor (**D2TO**) applying the following equation:

$$\varepsilon_T(\text{donor}) = \varepsilon_T(\text{acceptor}) \cdot \frac{\Delta A_{MAX}(\text{donor})}{\Delta A_{MAX}(\text{acceptor})} \cdot f_D P_{TEW}$$

Eq. 2

Prior to dealing with Eq.3, it is important to define:

- ΔA_{MAX} as the maximum value of the decay curve recorded at the maximum wavelength of the T_0 - T_n spectrum (λ_T);
- f_D as the fraction of absorbed light by the donor, defined by Eq. 3:

$$f_D = \frac{A_D \left(1 - 10^{-A_{TOT}} \right)}{A_{TOT} \left(1 - 10^{-A_D} \right)}$$

Eq. 3

where A_{TOT} is the absorbance of the solution containing both the donor and the acceptor and A_D the absorbance at 355 nm of the solution containing the donor alone (cuvette optical length 1 cm);

- P_{TE} as the energy transfer probability, given by:

$$P_{TE} = \frac{k'_{TD} - k_{TD}}{k'_{TD}}$$

Eq. 4

where k'_{TD} and k_{TD} are the decay kinetic constants of the donor in the presence and in the absence of the acceptor, respectively;

- W as the correction factor accounting for triplet decay rate constants of the donor (k'_{TD}) and acceptor (k_{TA}):

$$W = \exp\left(-\frac{\ln\left(\frac{k'_{TD}}{k_{TA}}\right)}{\left(\frac{k'_{TD}}{k_{TA}}\right) - 1}\right)$$

Eq. 5

The experimental procedure required the acquisition of:

1. The triplet decay kinetics of the donor and the acceptor separately, at their relative maximum wavelengths (490 and 465 nm respectively);
2. The decay kinetic of the solution containing the energy donor alone at the λ_T of the acceptor (465 nm);
3. The kinetics of the mixture containing both the donor and the acceptor at the triplet maxima of the two species (490 and 465 nm)

in the same experimental conditions.

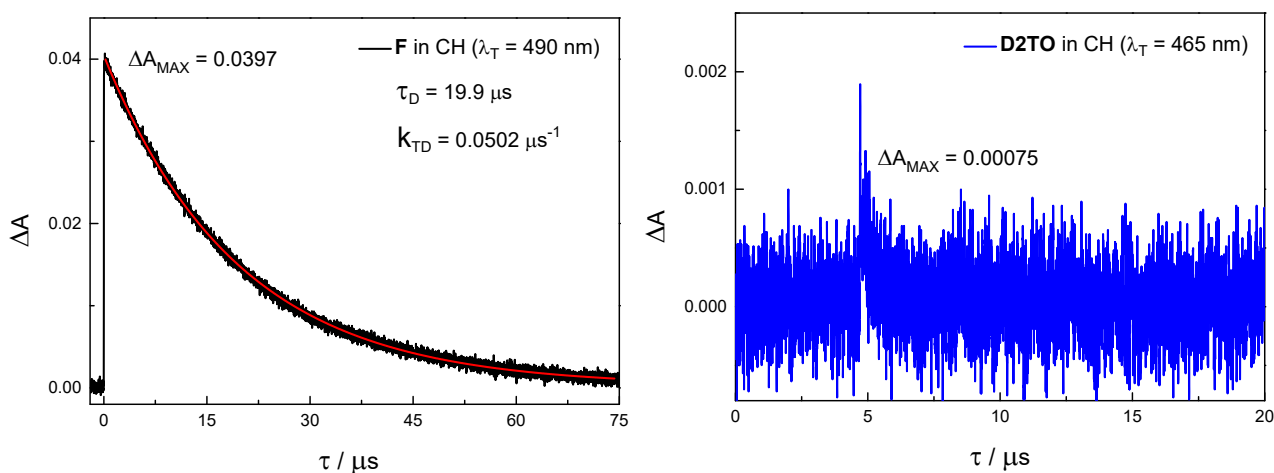


Figure S11: Kinetics obtained by ns transient absorption measurements ($\lambda_{exc} = 355$ nm) for the donor (**F**, $A_D = 0.9550$, $c = 1.93 \times 10^{-5}$ M), left, and the acceptor (**D2TO**) recorded at their relative λ_T in de-aerated conditions.

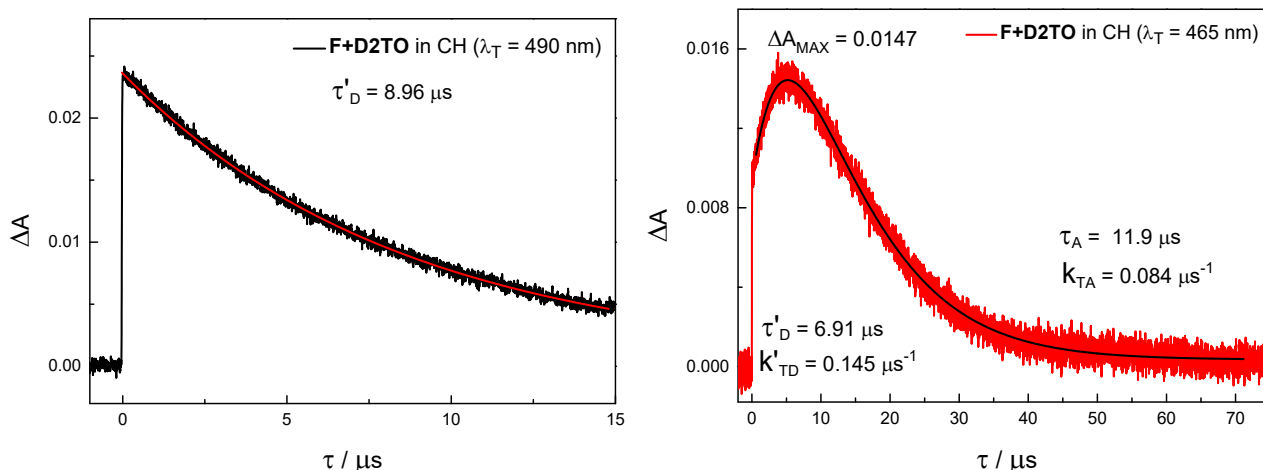


Figure S12: Kinetics obtained by ns transient absorption measurements ($\lambda_{exc} = 355 \text{ nm}$) for the **F/D2TO** ($A_{TOT} = 1.2596$) mixture recorded at their relative λ_T in de-aerated conditions.

According to the experimental results above and applying Eq.2:

$$\begin{aligned} \varepsilon_T(\text{donor}) &= \varepsilon_T(\text{acceptor}) \frac{\Delta A_{MAX}(\text{donor})}{\Delta A_{MAX}(\text{acceptor})} \cdot f_D \rho_{TE} W = 53000 \text{ M}^{-1} \text{ cm}^{-1} \frac{0.0397}{0.0147} \cdot 0.806 \times 0.6 \\ & \text{M}^{-1} \text{ cm}^{-1} \end{aligned}$$

Table S4: Molar absorption coefficients of first triplet excited state (ε_T) of compounds **F**, **AF** and **NF** in CH.

	F	AF	NF
λ_T / nm	500	530	530
$\varepsilon_T / \text{M}^{-1} \text{cm}^{-1}$	35500	28000*	31000*

*from ref.¹

3.3.3 Determination of the triplet quantum yields

Analogously to **AF** and **NF** in ref.¹, the triplet quantum yields (Φ_T) of compound **F** in different solvents were measured by quantitative experiments with two reference compounds using an actinometry approach: thioxhanten-9-one, **TX**, in MeCN ($\Phi_T = 0.66$ and $\varepsilon_T = 30000 \text{ M}^{-1} \text{ cm}^{-1}$ at 630 nm)^{5,6} and anthracene, **A**, in CH ($\Phi_T = 0.71$ and $\varepsilon_T = 45500 \text{ M}^{-1} \text{ cm}^{-1}$ at 422 nm)⁷. Eq. 6, stated below, has then been applied to determine the triplet quantum yield:

$$\frac{\Delta A_{MAX}(\text{sample})/A_{\text{sample}}}{\Delta A_{MAX}(\text{reference})/A_{\text{reference}}} = \frac{\phi_T \cdot \varepsilon_T(\text{sample})}{\phi_T \cdot \varepsilon_T(\text{reference})}$$

Eq. 6

In practise, the kinetics of compound **F** in different solvents ($\lambda_T = 490$ in CH and 500 nm in Tol, EtAc and DMF) and **TX** in MeCN ($\lambda_T = 630$ nm) and **A** in CH ($\lambda_T = 422$ nm) at the λ_T of the maximum triplet absorption were recorded in the same experimental conditions of laser power, time and flux rate of pure Nitrogen purged for the de-aeration process. We carefully tuned the laser power and verified the mono-exponential fitting of each acquired kinetic in order to avoid disturbing phenomena as triplet-triplet annihilation or second-order effects. In this manner, the ΔA_{MAX} has been estimated and manipulated in Eq.6. In addition, the triplet absorption coefficient was considered to be independent from solvent effect and thus kept constant when going from CH to DMF. The determination of Φ_T of **F** in all solvents is shown as representative examples of the applied procedure. Taking advantage of two different references it was

possible to monitor the reliability of the results by mutually checking whether one standard could provide the literature Φ_T value for the other one. For each reported measurement this relative error was <15%.

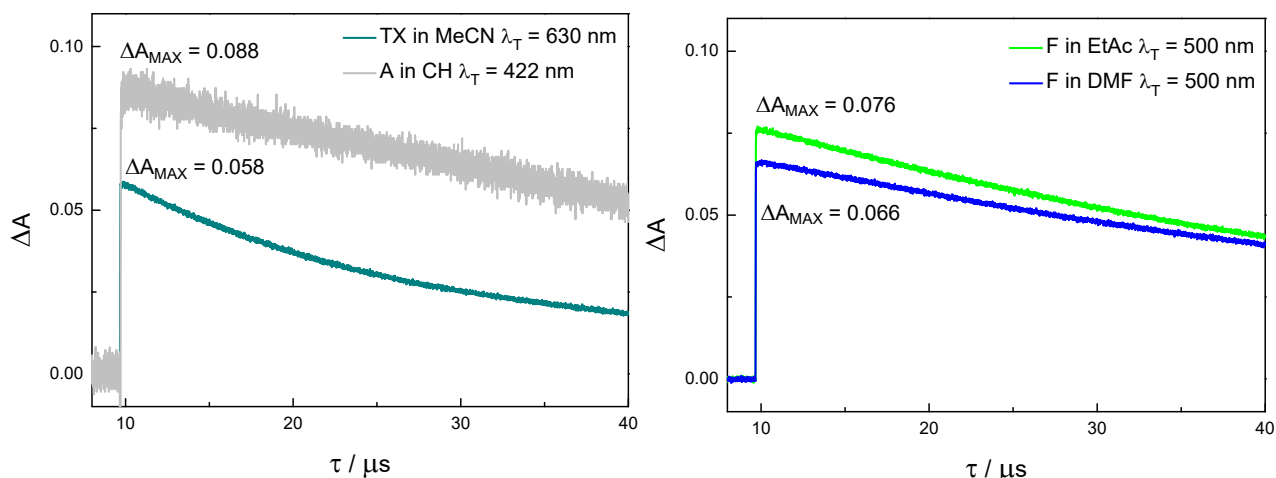


Figure S13: Kinetics obtained by ns transient absorption measurements ($\lambda_{exc} = 355$ nm) for the references (left) and compound **F** (right) at their λ_T in de-aerated conditions.

Table S5: Experimental details for the determination of Φ_T of compound **F** in solvents of different polarity ($\lambda_{exc} = 355$ nm). The last two lines refer to the representative example of mutual check of the actinometry approach ($\Phi_T = 0.66$ in the case of TX in MeCN and $\Phi_T = 0.71$ for A in CH).

Sample	$A_{355,S}$	$\lambda_{T,S} / \text{nm}$	$\Delta A_{MAX,S}$	Ref.	$A_{355,R}$	$\lambda_{T,R} / \text{nm}$	$\Delta A_{MAX,R}$	$\Phi_T \times \epsilon_T / \text{M}^{-1}\text{cm}^{-1}$	Φ_T
F in CH	0.294	490	0.122	TX in MeCN	0.301	630	0.061	40308	1.14
	0.349	490	0.082	A in CH	0.314	422	0.094	25146	0.71
F in Tol	0.306	500	0.080	TX in MeCN	0.296	630	0.055	27840	0.78
	0.335	500	0.097	A in CH	0.326	422	0.098	31144	0.88
F in EtAc	0.305	500	0.076	TX in MeCN	0.305	630	0.058	25943	0.73
	0.305	500	0.076	A in CH	0.302	422	0.088	27671	0.78
F in DMF	0.280	500	0.066	TX in MeCN	0.305	630	0.058	24500	0.69
	0.280	500	0.066	A in CH	0.302	422	0.088	26132	0.74
TX in MeCN	0.305	630	0.058	A in CH	0.302	422	0.088	21119	0.70
A in CH	0.302	422	0.088	TX in MeCN	0.305	630	0.058	30288	0.67

Table S6: Triplet properties of compound **F** in solvents of different polarity obtained by ns flash photolysis ($\lambda_{exc} = 355$ nm). The averaged values of triplet quantum yields obtained considering also additional independent replicas are reported.

solvent	λ_T / nm	$\tau_T(\text{air}) / \mu\text{s}$	$\tau_T(\text{N}_2) / \mu\text{s}$	$\epsilon_T / \text{M}^{-1}\text{cm}^{-1}$	$\Phi_T \times \epsilon_T / \text{M}^{-1}\text{cm}^{-1}$	Φ_T
CH	490	0.25	16.0	35500	33450	0.94
Tol	500	0.21	7.5		30550	0.86
EtAc	500	0.17	28.8		26800	0.76
DMF	500	0.21	48.4		25300	0.72

3.3.4 Concentration effect on the triplet quantum yields

The same experimental method was applied to measure the triplet quantum yields of the fluorene derivatives at different concentration levels. The study of the concentration effect is intrinsically limited by the experimental

technique. Therefore, a narrow range (from $A_{355} \approx 0.1$ up to $A_{355} = 1$, condition of total absorbance) was analyzed, restraining the concentration interval between 2.5×10^{-6} and 2.5×10^{-5} M, considering the ε_G shown in Table S8. Due to the lower absorption coefficient of **F** in CH it was possible to reach $\approx 9 \times 10^{-5}$ M as upper concentration limit. The concentration effect on triplet yield of **F** in Tol is reported as representative example.

Table S7: Molar absorption coefficients at 355 nm for the ground state of investigated samples in CH and Tol.

$\varepsilon_G / M^{-1}cm^{-1}$ at 355 nm		
sample	CH	Tol
F	11350	38990
AF	43320	41030
NF	43300	42000

Table S8: Experimental details for the determination of the concentration effect on Φ_T for compound **F** in Tol.

sample	C / M	A_{355}	ΔA_{MAX}	Ref.	A_{355}	ΔA_{MAX}	$\Phi_T \times \varepsilon_T$	Φ_T
NF in Tol	2×10^{-6}	0.1007	0.0602	TX in MeCN	0.0965	0.0472	24200	0.68
				A in CH	0.1130	0.0790	27624	0.78
							25912	0.73
TX in MeCN		0.0965	0.0472	A in CH	0.1130	0.0790	22600	0.75
A in CH		0.1130	0.0790	TX in MeCN	0.0965	0.0472	28300	0.63
NF in Tol	7×10^{-6}	0.3346	0.0970	A in CH	0.3259	0.0980	31144	0.88
				TX in MecN	0.2960	0.0549	27840	0.78
							30550	0.86
TX in MeCN		0.2960	0.0549	A in CH	0.3259	0.0980	19925	0.66
A in CH		0.3259	0.0980	TX in MeCN	0.2960	0.0549	32101	0.71
NF in Tol	1×10^{-5}	0.5040	0.1086	TX in MeCN	0.5360	0.0646	35399	1.00
				A in CH	0.5520	0.1010	38044	1.07
							36722	1.03
TX in MeCN		0.5360	0.0646	A in CH	0.5520	0.1010	21279	0.71
A in CH		0.5520	0.1010	TX in MeCN	0.5360	0.0646	30059	0.67
NF in Tol	2×10^{-5}	1.0160	0.1262	TX in MeCN	1.0770	0.0682	38838	1.09
				A in CH	1.0980	0.1040	42365	1.19
							40602	1.14
TX in MeCN		1.0770	0.0682	A in CH	1.0980	0.1040	21598	0.72
A in CH		1.0980	0.1040	TX in MeCN	1.0770	0.0682	29616	0.66

*bold values are the averaged triplet quantum yields obtained by several independent replicas.

Also, the concentration effect on triplet lifetimes was considered and reported in Table S9.

Table S9. Concentration effect on triplet lifetime (τ_T).

C / M	$\tau_T / \mu s$					
	F		AF		NF	
	CH	Tol	CH	Tol	CH	Tol
2.5×10^{-6}	152*	152	151	53	45	144
1.3×10^{-5}	90 [#]	109	97	40	47	120
2.5×10^{-5}	29 [§]	38	60	33	15	87

* 7×10^{-6} ; [#] 2.5×10^{-5} ; [§] 9×10^{-5} M.

Table S10. Overview of the fractions of the total triplet yield estimated for the ISC and the SF processes separately.

		$\Phi_{T,ISC}^a$	$\Phi_{T,exp}^b$	$\Phi_{T,SF}^c$
CH	F	0.66	0.94	0.28
	AF	0.46	1.17	0.71
	NF	0.57	1.45	0.88
Tol	F	0.73	1.14	0.41
	AF	0.53	0.87	0.34
	NF	0.52	1.10	0.58

^a $\Phi_{T,ISC}$ obtained as the triplet yield of the isolated monomer from the values in the most diluted solution (ca. 2.5×10^{-6} M) and at cryogenic temperature; ^b $\Phi_{T,exp}$ is the triplet yield measured in 2.5×10^{-5} M solution (see Table 1); ^c $\Phi_{T,SF}$ obtained as $\Phi_{T,exp} - \Phi_{T,ISC}$.

3.4 Femtosecond transient absorption and fluorescence up conversion experiments

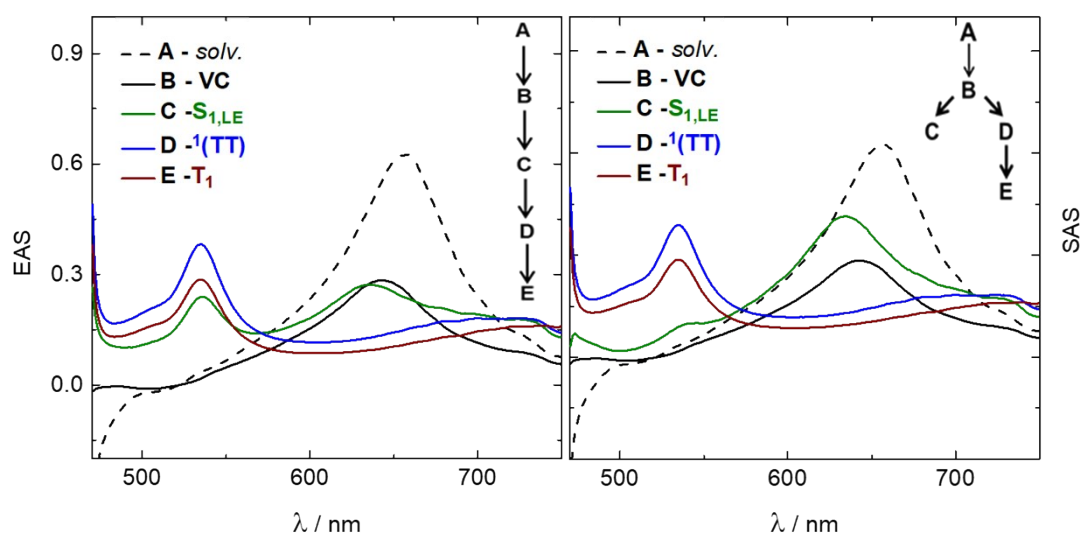


Figure S14. Comparison between EAS (left), obtained by Global analysis with a consecutive kinetic model, and SAS (right), given by Target analysis using a branched kinetic model, for compound **NF** in Tol.

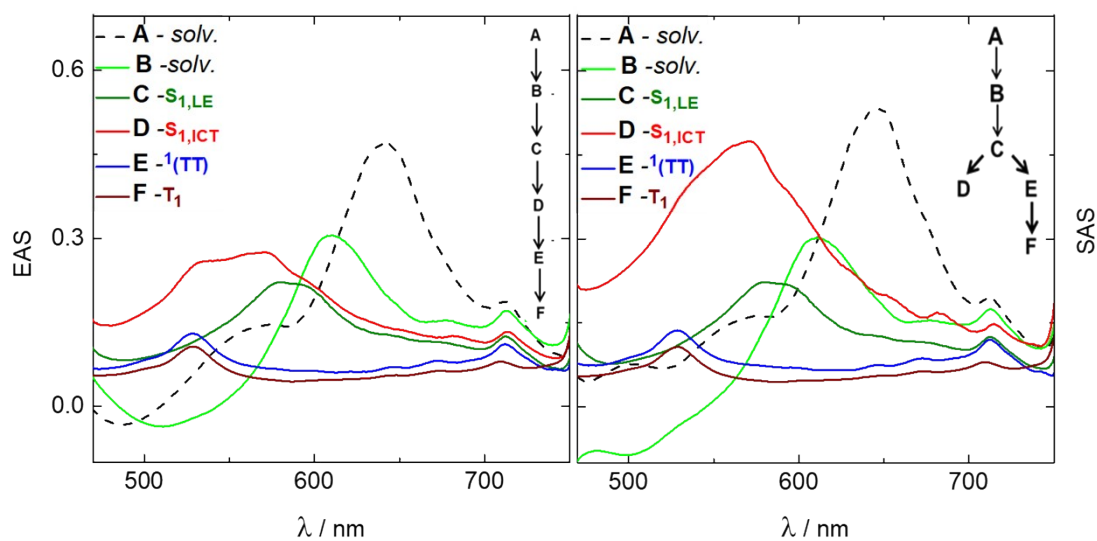


Figure S15. Comparison between EAS (left), obtained by Global analysis with a consecutive kinetic model, and SAS (right), given by Target analysis using a branched kinetic model, for compound **NF** in EtAc.

Table S11. Global fit of fs TA measurements of **F**, **NF** and **AF** (ca. 1×10^{-4} M) in solvents of different polarity obtained by pump-probe technique ($\lambda_{\text{exc}} = 266$ nm for **F** and $\lambda_{\text{exc}} = 400$ nm for **NF** and **AF**). In the case of **F** the choice of the solvent was limited to CH and MeCN, which do not absorb the UV light at 266 nm.

solvent	F			AF			NF		
	τ / ps	λ /nm	transient	τ / ps	λ /nm	transient	τ / ps	λ /nm	transient
CH	3.2	570(-)	V.C.	0.20	670	V.C.	0.50	650	V.C.
	127	575	$S_{1,LE}$	77	670	$S_{1,LE}$	5.6	525 (-) 715(-)	$S_{1,LE}$
	640	<520, 600	$^1(TT)$	620	525 >700	$^1(TT)$	400	525 715	$^1(TT)$
	rest	<520	T_1	rest	525 >700	T_1	rest	525 710	T_1
Tol							0.74	660	<i>solv.</i>
				3.7	670	<i>solv.</i>	7.9	650	V.C.
				205	675	$S_{1,LE}$	45	630	$S_{1,LE}$
				520	530	$^1(TT)$	390	530 675	$^1(TT)$
				rest	530	T_1	rest	530 725	T_1
EtAc							0.53	650	<i>solv.</i>
				1.0	655 520	<i>solv.</i>	1.5	620	<i>solv.</i>
				5.8	645	$S_{1,LE}$	7.6	530 (-) 715 (-)	$S_{1,LE}$
				713	630	$S_{1,ICT}$	42	575	$S_{1,ICT}$
				-	-	-	100	530 715	$^1(TT)$
				rest	530	T_1	rest	525 710	T_1
DMF/ MeCN*	3.0	570(-)	V.C.	0.63	650	<i>solv.</i>	0.59	655	<i>solv.</i> , $S_{1,LE}$
	114	570	$S_{1,LE}$	2.2	645	$S_{1,LE}$	2.4	555	<i>solv.</i> , $S_{1,ICT}$
	810	<510 585	$^1(TT)$	30	575	$S_{1,ICT}$	280	535 670	$^1(TT)$
	rest	<520	T_1	-		-	rest	535 710	T_1

*DMF for the case of **NF** and **AF**; MeCN for the case of **F**.

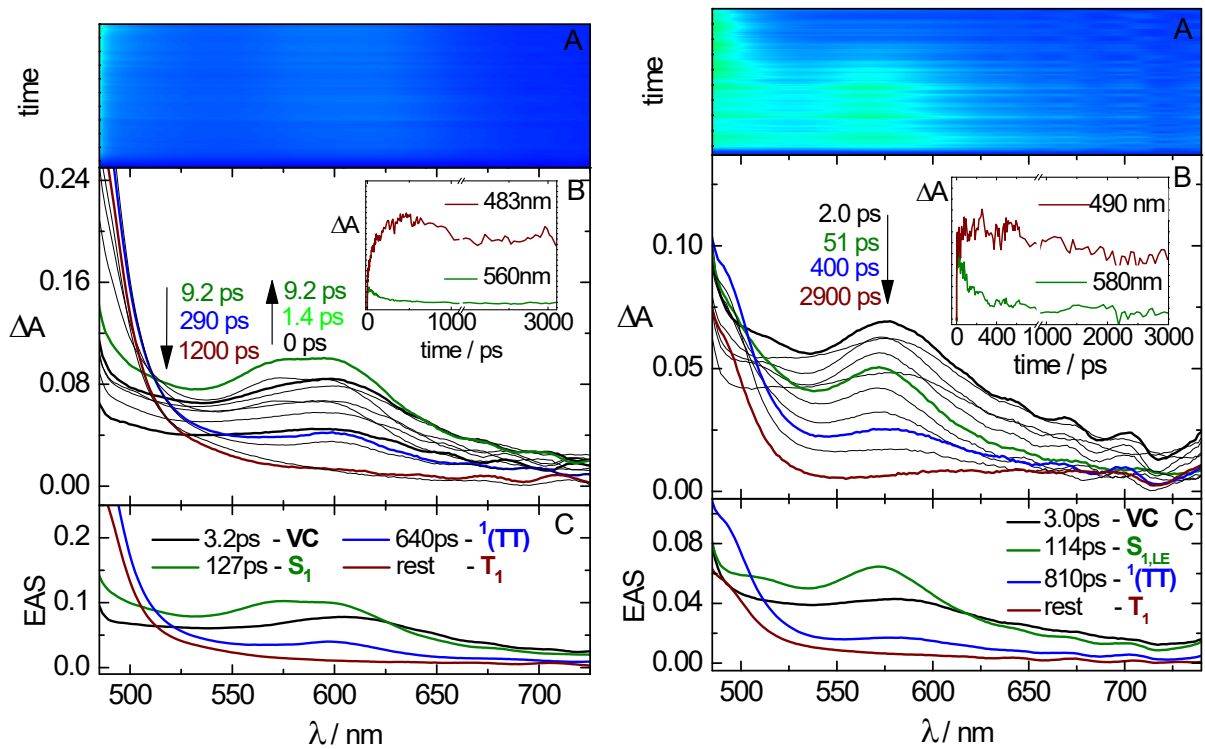


Figure S16. Femtosecond transient absorption measurements of F in CH (left) and MeCN (right) solutions (ca. 1×10^{-4} M) by exciting at $\lambda_{\text{pump}} = 266$ nm.

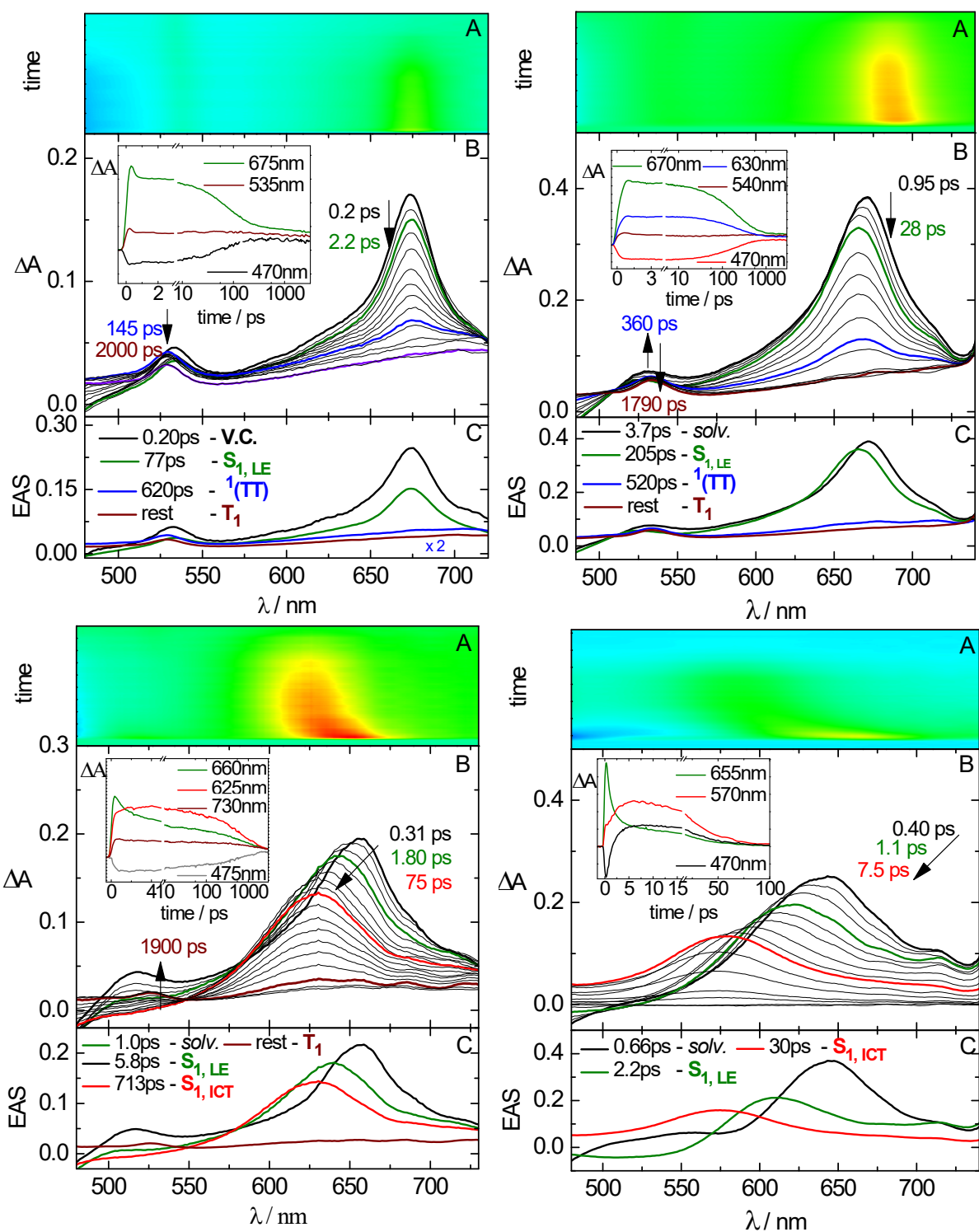


Figure S17. Femtosecond transient absorption measurements of AF in CH (top left), Tol (top right), in EtAc (bottom left) and DMF (bottom right) solutions (ca. $1 \times 10^{-4} \text{ M}$) with $\lambda_{\text{pump}} = 400 \text{ nm}$.

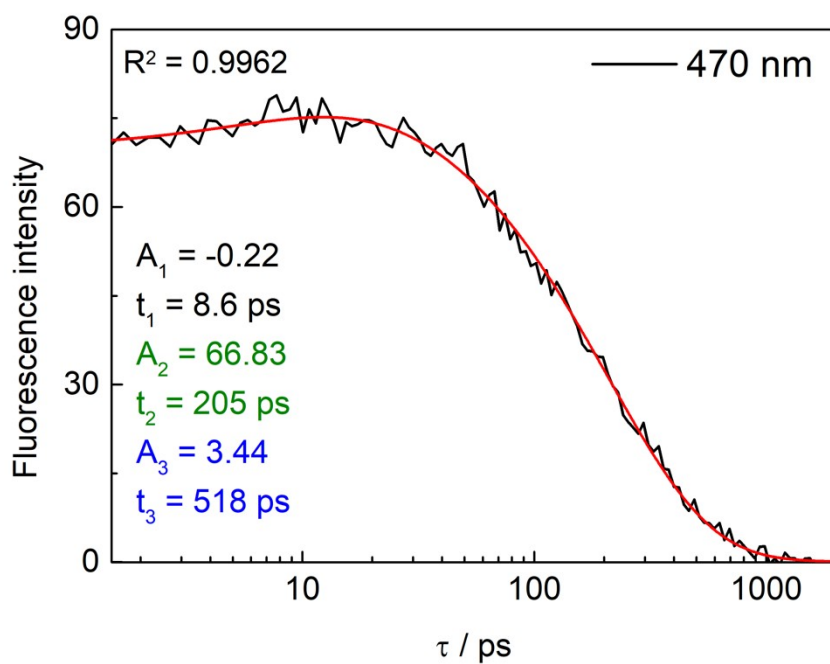


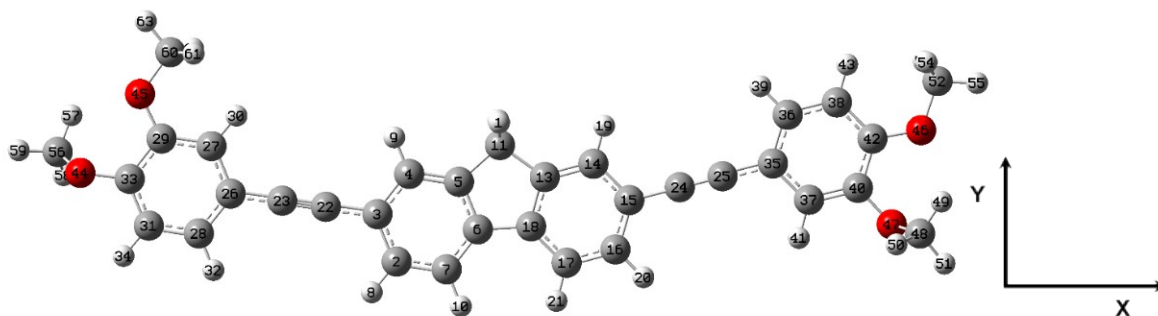
Figure S18. Fluorescence kinetics at 470 nm obtained for **AF** in Tol from the fluorescence up conversion measurements (ca. 1×10^{-4} M) with $\lambda_{\text{pump}} = 400$ nm and relative fitting.

Table S12. Global fit of fs TA measurements of **NF** in CH obtained in solutions characterized by different concentrations ($\lambda_{\text{exc}} = 400$; corresponding ground state absorbance values between 0.6 and 0.025 at 400 nm in a 2 mm cuvette).

Concentration / M	1×10^{-4} M		1.8×10^{-5} M		8×10^{-6} M		4×10^{-6} M	
	τ / ps	transient	τ / ps	transient	τ / ps	transient	τ / ps	transient
NF in CH	0.50	V.C.	0.60	V.C.	0.47	V.C.	0.49	V.C.
	5.6	$S_{1,LE}$	5.3	$S_{1,LE}$	6.0	$S_{1,LE}$	6.0	$S_{1,LE}$
	400	${}^1(\text{TT})$	400	${}^1(\text{TT})$	595	${}^1(\text{TT})$	645	${}^1(\text{TT})$
	rest	T_1	rest	T_1	rest	T_1	rest	T_1

4. Quantum mechanical calculations

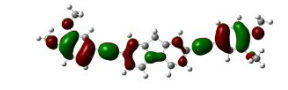
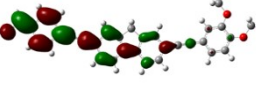
Table S13. Cartesian coordinates of optimized S_0 (shown below), S_1 and T_1 geometries of compound **F** in CH calculated by the CAM-B3LYP/6-31+G(d,p)//CAM-B3LYP/6-31+G(d,p) model.



n. atom	Atomic n.	Coordinates S_0 /Angstrom			Coordinates S_1 /Angstrom			Coordinates T_1 /Angstrom		
		X	Y	Z	X	Y	Z	X	Y	Z
1	1	-0.196844	1.510685	0.901058	-0.188595	1.520765	0.945409	-0.188595	1.520765	0.945409
2	6	-3.005808	-2.321216	-0.011625	-3.00057	-2.293398	-0.038974	-3.00057	-2.293398	-0.038974
3	6	-3.513147	-1.024437	-0.006036	-3.52792	-0.99125	0.017266	-3.52792	-0.99125	0.017266
4	6	-2.654341	0.08435	-0.002547	-2.656622	0.111116	0.046322	-2.656622	0.111116	0.046322
5	6	-1.290375	-0.133131	-0.004777	-1.291063	-0.104624	0.018883	-1.291063	-0.104624	0.018883
6	6	-0.770892	-1.455998	-0.010417	-0.772693	-1.409166	-0.037406	-0.772693	-1.409166	-0.037406
7	6	-1.626268	-2.54753	-0.013827	-1.628975	-2.50712	-0.066383	-1.628975	-2.50712	-0.066383
8	1	-3.691565	-3.173637	-0.01438	-3.683049	-3.1359	-0.060812	-3.683049	-3.1359	-0.060812
9	1	-3.064703	1.098012	0.001735	-3.065801	1.11544	0.089853	-3.065801	1.11544	0.089853
10	1	-1.234263	-3.568608	-0.018092	-1.239184	-3.519233	-0.109741	-1.239184	-3.519233	-0.109741
11	6	-0.162906	0.864462	-0.002131	-0.165418	0.90281	0.040656	-0.165418	0.90281	0.040656
12	1	-0.198788	1.517633	-0.90023	-0.213702	1.586894	-0.814146	-0.213702	1.586894	-0.814146
13	6	1.064942	-0.006609	-0.006802	1.063628	0.025663	-0.009908	1.063628	0.025663	-0.009908
14	6	2.397763	0.355764	-0.006774	2.397321	0.39116	-0.015661	2.397321	0.39116	-0.015661
15	6	3.370297	-0.654723	-0.011579	3.384179	-0.608144	-0.067678	3.384179	-0.608144	-0.067678
16	6	3.004829	-1.998376	-0.016702	3.002362	-1.960717	-0.112922	3.002362	-1.960717	-0.112922
17	6	1.657487	-2.371174	-0.016651	1.662576	-2.324691	-0.107001	1.662576	-2.324691	-0.107001
18	6	0.690158	-1.377511	-0.011691	0.691196	-1.328063	-0.05532	0.691196	-1.328063	-0.05532
19	1	2.697254	1.407536	-0.003023	2.694012	1.434606	0.018976	2.694012	1.434606	0.018976
20	1	3.777947	-2.772435	-0.020689	3.77294	-2.722735	-0.153128	3.77294	-2.722735	-0.153128
21	1	1.377164	-3.428367	-0.0205	1.386183	-3.373756	-0.142568	1.386183	-3.373756	-0.142568
22	6	-5.001795	-0.804207	-0.003649	-4.94345	-0.790803	0.044621	-4.94345	-0.790803	0.044621
23	6	-6.194618	-0.6281	-0.001733	-6.142337	-0.62251	0.067874	-6.142337	-0.62251	0.067874
24	6	4.826803	-0.276465	-0.011308	4.769081	-0.25271	-0.074703	4.769081	-0.25271	-0.074703
25	6	5.993686	0.026545	-0.011061	5.942001	0.048415	-0.081246	5.942001	0.048415	-0.081246
26	6	-7.683019	-0.409597	0.000657	-7.559192	-0.427293	0.094554	-7.559192	-0.427293	0.094554
27	6	-8.197413	0.880197	0.006155	-8.083136	0.875694	0.154968	-8.083136	0.875694	0.154968
28	6	-8.544516	-1.489411	-0.002712	-8.429371	-1.519239	0.065519	-8.429371	-1.519239	0.065519
29	6	-9.576967	1.12499	0.009078	-9.456402	1.083488	0.185166	-9.456402	1.083488	0.185166
30	1	-7.500891	1.717676	0.009491	-7.396855	1.71138	0.187567	-7.396855	1.71138	0.187567
31	6	-9.91463	-1.275141	-0.000884	-9.803902	-1.305671	0.086061	-9.803902	-1.305671	0.086061
32	1	-8.148408	-2.508576	-0.007226	-8.031206	-2.526351	0.024471	-8.031206	-2.526351	0.024471
33	6	10.480678	0.002358	0.005055	10.327247	-0.023205	0.139539	10.327247	-0.023205	0.139539
34	1	10.583481	-2.140425	-0.004038	10.497945	-2.139065	0.066853	10.497945	-2.139065	0.066853
35	6	7.449795	0.404583	-0.010745	7.327646	0.39993	-0.088697	7.327646	0.39993	-0.088697

36	6	7.820792	1.735889	-0.005671	7.731276	1.736197	-0.039309	7.731276	1.736197	-0.039309
37	6	8.424211	-0.585476	-0.015448	8.315461	-0.597254	-0.144466	8.315461	-0.597254	-0.144466
38	6	9.166139	2.069941	-0.007214	9.081311	2.073873	-0.053374	9.081311	2.073873	-0.053374
39	1	7.058548	2.519956	-0.003042	6.984066	2.520497	0.006546	6.984066	2.520497	0.006546
40	6	9.78964	-0.29474	-0.013834	9.658386	-0.270473	-0.155358	9.658386	-0.270473	-0.155358
41	1	8.113687	-1.633851	-0.019015	8.040118	-1.644996	-0.187801	8.040118	-1.644996	-0.187801
42	6	10.172214	1.092332	-0.011508	10.05648	1.080591	-0.117902	10.05648	1.080591	-0.117902
43	1	9.439817	3.12442	-0.006101	9.363081	3.118579	-0.022807	9.363081	3.118579	-0.022807
44	8	-11.921036	-0.123954	0.006324	-11.683593	0.141855	0.219628	-11.683593	0.141855	0.219628
45	8	-9.95854	2.491313	0.015545	-10.044682	2.305318	0.267385	-10.044682	2.305318	0.267385
46	8	11.507206	1.572623	-0.019244	11.392179	1.313107	-0.157619	11.392179	1.313107	-0.157619
47	8	10.538496	-1.530089	-0.019444	10.585848	-1.272137	-0.272814	10.585848	-1.272137	-0.272814
48	6	11.952075	-1.687301	0.123373	11.365731	-1.525174	0.896216	11.365731	-1.525174	0.896216
49	1	12.460442	-1.274678	-0.72605	11.953064	-0.64654	1.174222	11.953064	-0.64654	1.174222
50	1	12.290166	-1.217185	1.027009	10.718509	-1.821533	1.729156	10.718509	-1.821533	1.729156
51	1	12.156305	-2.745789	0.177817	12.034132	-2.348855	0.644905	12.034132	-2.348855	0.644905
52	6	11.618855	3.000338	-0.009698	11.844394	2.658282	-0.15435	11.844394	2.658282	-0.15435
53	1	11.146264	3.415935	-0.885951	11.464706	3.204349	-1.024138	11.464706	3.204349	-1.024138
54	1	11.154131	3.402817	0.876855	11.545551	3.174556	0.764057	11.545551	3.174556	0.764057
55	1	12.665532	3.257208	-0.012584	12.931087	2.607243	-0.204797	12.931087	2.607243	-0.204797
56	6	-12.895799	0.920952	0.011705	-12.306011	0.714777	-0.931359	-12.306011	0.714777	-0.931359
57	1	-12.794468	1.520412	0.895476	-11.925737	1.720724	-1.123716	-11.925737	1.720724	-1.123716
58	1	-12.796119	1.527954	-0.867094	-12.142522	0.07834	-1.808072	-12.142522	0.07834	-1.808072
59	1	-13.869429	0.45492	0.010623	-13.372352	0.760694	-0.709736	-13.372352	0.760694	-0.709736
60	6	-8.857839	3.407724	0.018466	-9.212006	3.451028	0.350515	-9.212006	3.451028	0.350515
61	1	-8.252167	3.25769	0.898596	-8.575262	3.412825	1.240579	-8.575262	3.412825	1.240579
62	1	-8.254038	3.265556	-0.86425	-8.588229	3.553813	-0.543827	-8.588229	3.553813	-0.543827
63	1	-9.253159	4.410323	0.023358	-9.885309	4.304	0.423204	-9.885309	4.304	0.423204

Table S14. Absorption wavelengths (λ), oscillator strength (f_{os}) and molecular orbitals in CH (CPCM) starting from S_0 optimized geometry, calculated by the CAM-B3LYP/6-31+G(d,p)//CAM-B3LYP/6-31+G(d,p) model, together with the experimental absorption maxima.

Comp.d	Transition	λ_{th}/nm	f_{os}	MOs	%	λ_{exp}/nm	MOs	
F	$S_0 \rightarrow S_1$	343	2.7970	HOMO \rightarrow LUMO	86	349	 O HOM	 LUMO
	$S_0 \rightarrow S_2$	289	0.0824	HOMO-1 \rightarrow LUMO	52		 HOMO-1	 LUMO
AF	$S_0 \rightarrow S_1$	358	2.8647	HOMO \rightarrow LUMO	51	364	 HOMO	 LUMO

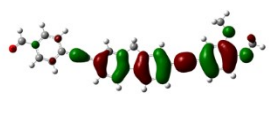
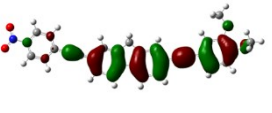
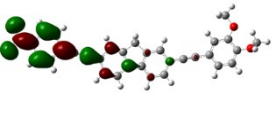
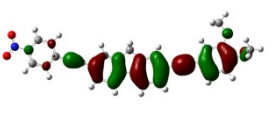
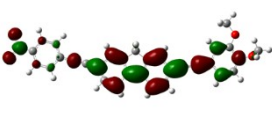
Comp.d	Transition	λ_{th}/nm	f_{os}	MOs	%	λ_{exp}/nm	MOs	
	$S_0 \rightarrow S_3$	306	0.0977	HOMO \rightarrow LUMO+1	42			
	$S_0 \rightarrow S_1$	365	2.5104	HOMO \rightarrow LUMO	50	370		
NF	$S_0 \rightarrow S_3$	310	0.2987	HOMO \rightarrow LUMO+1	53	310		

Table S15. Absorption wavelengths (λ), oscillator strength (f_{os}) and molecular orbitals of **F** in CH (CPCM) starting from T_1 optimized geometry, calculated by the CAM-B3LYP/6-31+G(d,p)//CAM-B3LYP/6-31+G(d,p) model, together with the experimental absorption maxima.

Transition	λ_{th}/nm	f_{os}	MO	%	λ_{exp}/nm
$T_1 \rightarrow T_2$	1612	0.0216	SUMO \rightarrow SUMO+1 SOMO-1 \rightarrow SOMO	43 55	
$T_1 \rightarrow T_3$	672	0.0208	SUMO \rightarrow SUMO+2 SUMO \rightarrow SUMO+3	52 25	
$T_1 \rightarrow T_4$	622	2.5086	SUMO \rightarrow SUMO+1 SOMO-1 \rightarrow SOMO	44 38	490
$T_1 \rightarrow T_5$	573	0.4595	SOMO-5 \rightarrow SOMO	60	
$T_1 \rightarrow T_6$	538	0.0077	SOMO-2 \rightarrow SOMO	49	
$T_1 \rightarrow T_7$	475	0.0071	SOMO-7 \rightarrow SOMO	78	
$T_1 \rightarrow T_8$	457	0.0126	SUMO \rightarrow SUMO+12 SOMO-5 \rightarrow SOMO	23 23	
$T_1 \rightarrow T_9$	441	0.0747	SUMO \rightarrow SUMO+10 SOMO-3 \rightarrow SOMO	9 18	
$T_1 \rightarrow T_{10}$	406	0.0336	SUMO \rightarrow SUMO+3 SOMO-2 \rightarrow SOMO	29 37	
$T_1 \rightarrow T_{11}$	394	0.0000	SOMO-9 \rightarrow SOMO SOMO-8 \rightarrow SOMO	30 56	

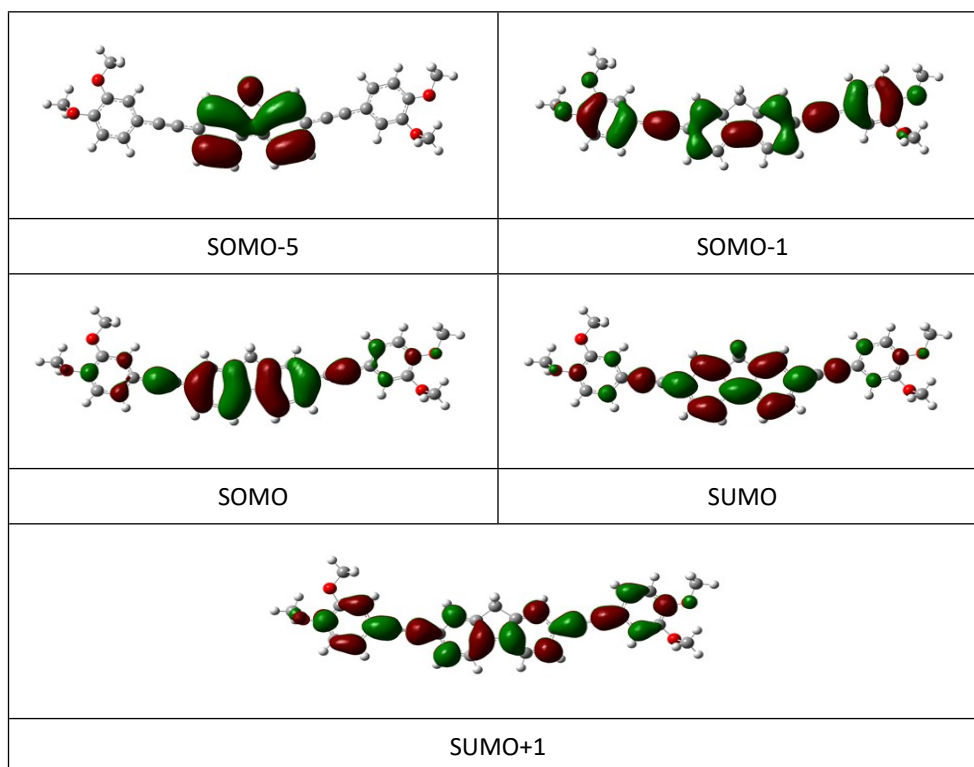


Figure S19. Molecular orbitals of compounds **F** in CH calculated by the CAM-B3LYP/6-31+G(d,p)//CAM-B3LYP/6-31+G(d,p) model.

Table S16. Absorption wavelengths (λ), oscillator strength (f_{os}) and molecular orbitals of **AF** in CH (CPCM) starting from T_1 optimized geometry, calculated by the CAM-B3LYP/6-31+G(d,p)//CAM-B3LYP/6-31+G(d,p) model, together with the experimental absorption maxima.

Transition	λ_{th}/nm	f_{os}	MO	%	λ_{exp}/nm
$T_1 \rightarrow T_2$	1505	0.0226	SUMO \rightarrow SUMO+1	57	
$T_1 \rightarrow T_3$	686	2.1730	SUMO \rightarrow SUMO+1 SOMO-1 \rightarrow SOMO	27 48	720
$T_1 \rightarrow T_4$	597	0.0204	SOMO-7 \rightarrow SOMO SOMO-4 \rightarrow SOMO	30 22	
$T_1 \rightarrow T_5$	585	0.0000	SOMO-9 \rightarrow SOMO	82	
$T_1 \rightarrow T_6$	526	0.7537	SUMO \rightarrow SUMO+1 SUMO \rightarrow SUMO+2	15 13	525
$T_1 \rightarrow T_7$	481	0.0139	SUMO \rightarrow SUMO+3 SOMO-4 \rightarrow SOMO	47 17	
$T_1 \rightarrow T_8$	478	0.0007	SUMO \rightarrow SUMO+4 SOMO-6 \rightarrow SOMO	25 49	
$T_1 \rightarrow T_9$	474	0.0000	SOMO-5 \rightarrow SOMO SOMO-5 \rightarrow SUMO	50 24	
$T_1 \rightarrow T_{10}$	436	0.0842	SUMO \rightarrow SUMO+2 SOMO-2 \rightarrow SOMO	23 9	
$T_1 \rightarrow T_{11}$	422	0.0423	SUMO \rightarrow SUMO+4 SOMO-1 \rightarrow SOMO	9 9	

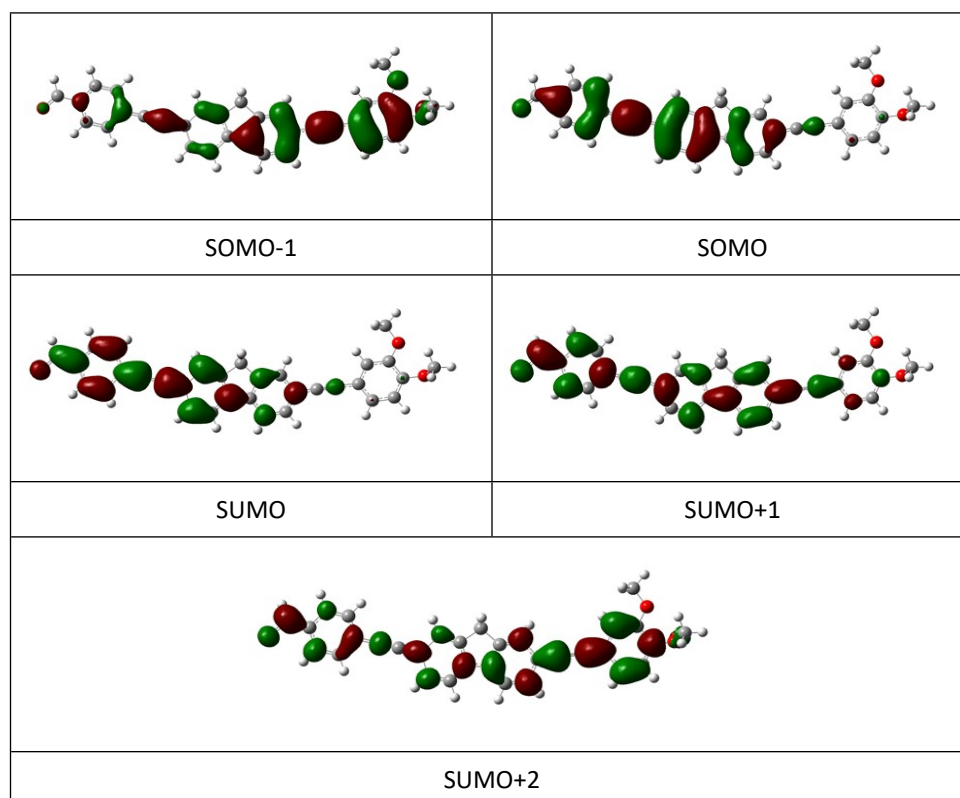


Figure S20. Molecular orbitals of compounds **AF** in CH calculated by the CAM-B3LYP/6-31+G(d,p)//CAM-B3LYP/6-31+G(d,p) model.

Table S17. Absorption wavelengths (λ), oscillator strength (f_{os}) and molecular orbitals of **NF** in CH (CPCM) starting from T_1 optimized geometry, calculated by the CAM-B3LYP/6-31+G(d,p)//CAM-B3LYP/6-31+G(d,p) model, together with the experimental absorption maxima.

Transition	λ_{th}/nm	f_{os}	MO	%	λ_{exp}/nm
$T_1 \rightarrow T_2$	1676	0.0979	SUMO \rightarrow SUMO+1	69	
$T_1 \rightarrow T_3$	794	2.0806	SOMO-1 \rightarrow SOMO	49	> 750
$T_1 \rightarrow T_4$	596	0.0000	SOMO-10 \rightarrow SOMO SOMO-8 \rightarrow SOMO	50 43	
$T_1 \rightarrow T_5$	579	0.0020	SOMO-6 \rightarrow SOMO SOMO-4 \rightarrow SOMO	41 26	
$T_1 \rightarrow T_6$	526	0.4162	SUMO \rightarrow SUMO+5 SOMO-5 \rightarrow SOMO	14 16	530
$T_1 \rightarrow T_7$	503	0.0057	SUMO \rightarrow SUMO+2 SOMO-5 \rightarrow SOMO	32 54	
$T_1 \rightarrow T_8$	480	0.2653	SUMO \rightarrow SUMO+2	41	
$T_1 \rightarrow T_9$	456	0.0806	SUMO \rightarrow SUMO+3	44	
$T_1 \rightarrow T_{10}$	445	0.0014	SUMO \rightarrow SUMO+5 SOMO-4 \rightarrow SOMO	35 21	
$T_1 \rightarrow T_{11}$	426	0.0955	SOMO \rightarrow SUMO+2 SOMO-7 \rightarrow SOMO	10 13	

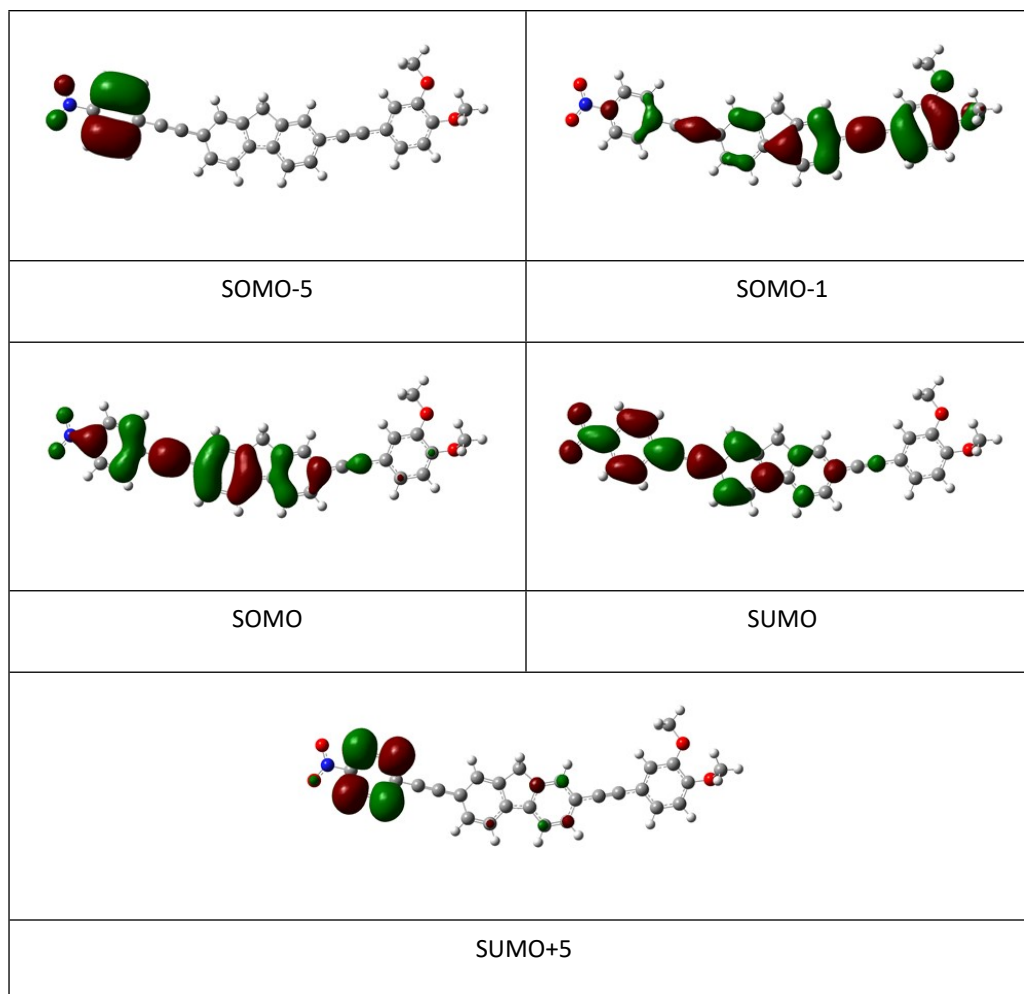


Figure S21. Molecular orbitals of compounds **NF** in CH calculated by the CAM-B3LYP/6-31+G(d,p)//CAM-B3LYP/6-31+G(d,p) model.

5. References

- 1 B. Carlotti, R. Flamini, A. Spalletti, A. Marrocchi and F. Elisei, *ChemPhysChem*, 2012, **13**, 724–735.
- 2 M. Montalti, A. Credi, L. Prodi and M. T. Gandolfi, *Handbook of Photochemistry*, CRC Press, Boca Raton, 3rd edn., 2006.
- 3 R. Schmidt, C. Tanielian, R. Dunsbach and C. Wolff, *Journal of Photochemistry and Photobiology A: Chemistry*, 1994, **79**, 11–17.
- 4 G. Bartocci, A. Spalletti, R. S. Becker, F. Elisei, S. Floridi and U. Mazzucato, *J. Am. Chem. Soc.*, 1999, **121**, 1065–1075.
- 5 X. Allonas, C. Ley, C. Bibaut, P. Jacques and J. P. Fouassier, *Chemical Physics Letters*, 2000, **322**, 483–490.
- 6 A. Samanta, B. Ramachandram and G. Saroja, *Journal of Photochemistry and Photobiology A: Chemistry*, 1996, **101**, 29–32.
- 7 I. Carmichael and G. L. Hug, *Journal of Physical and Chemical Reference Data*, 1986, **15**, 1–250.
- 8 B. Carlotti, A. Spalletti, M. Šindler-Kulyk and F. Elisei, *Physical Chemistry Chemical Physics*, 2011, **13**, 4519–4528.
- 9 A. Cesaretti, B. Carlotti, C. Clementi, R. Germani and F. Elisei, *Photochem. Photobiol. Sci.*, 2014, **13**, 509–520.
- 10 S. De Solis, A. Barbafina and F. Elisei, *Physical Chemistry Chemical Physics*, 2011, **13**, 2188–2195.
- 11 A. Cesaretti, B. Carlotti, G. Consiglio, T. Del Giacco, A. Spalletti and F. Elisei, *J. Phys. Chem. B*, 2015, **119**, 6658–6667.
- 12 A. Cesaretti, B. Carlotti, P. L. Gentili, R. Germani, A. Spalletti and F. Elisei, *Photochem. Photobiol. Sci.*, 2016, **15**, 525–535.
- 13 A. Cesaretti, B. Carlotti, F. Elisei, C. G. Fortuna and A. Spalletti, *Physical Chemistry Chemical Physics*, 2018, **20**, 2851–2864.
- 14 M. J. Frisch, G. W. Trucks, H. B. Schlegel, G. E. Scuseria, M. A. Robb, J. R. Cheeseman, G. Scalmani, V. Barone, G. A. Petersson and H. Nakatsuji, *Wallingford CT*.
- 15 S. Tortorella, M. M. Talamo, A. Cardone, M. Pastore and F. De Angelis, *J. Phys.: Condens. Matter*, 2016, **28**, 074005.
- 16 V. Barone and M. Cossi, *J. Phys. Chem. A*, 1998, **102**, 1995–2001.
- 17 F. Ortica, A. Romani and G. Favaro, *J. Phys. Chem. A*, 1999, **103**, 1335–1341.
- 18 Molecular Photochemistry. Von N. J. Turro. W. A. Benjamin, Inc., New York-Amsterdam 1965. 1. Aufl., XIII, 286 S., zahlr. Abb., geb. DM 55.– - Quinkert - 1967 - Angewandte Chemie - Wiley Online Library,

<https://onlinelibrary.wiley.com/doi/epdf/10.1002/ange.19670791617>, (accessed 4 October 2021).

19 A. J. Fry, R. S. H. Liu and G. S. Hammond, *J. Am. Chem. Soc.*, 1966, **88**, 4781–4782.